PHYSICAL REVIEW MATERIALS **6**, 044801 (2022)

Role of carbon in modifying the properties of superconducting hydrogen sulfide

Yuki Sakai,[1] James R. Chelikowsky,[1,2,3] and Marvin L. Cohen[4,5]
[1]*Center for Computational Materials, Oden Institute for Computational Engineering and Sciences,*
The University of Texas at Austin, Austin, Texas 78712, USA
[2]*McKetta Department of Chemical Engineering, The University of Texas at Austin, Austin, Texas 78712, USA*
[3]*Department of Physics, The University of Texas at Austin, Austin, Texas 78712, USA*
[4]*Department of Physics, University of California at Berkeley, Berkeley, California 94720, USA*
[5]*Materials Sciences Division, Lawrence Berkeley, National Laboratory, Berkeley, California 94720, USA*

(Received 19 December 2021; revised 25 February 2022; accepted 11 March 2022; published 4 April 2022)

We examine the role of adding carbon to influence the superconducting properties of hydrogen sulfide. We consider a number of unique structures employing a simulation cell containing carbon, hydrogen, and sulfur atoms with randomized atomic coordinates. We also reproduced some structures reported in the literature. In general, we find the presence of carbon atoms does not raise the superconducting transition temperature of hydrogen sulfide compounds. We discuss the origin of this trend through a detailed examination of structural and electronic properties of carbon-hydrogen-sulfur materials.

DOI: 10.1103/PhysRevMaterials.6.044801

I. INTRODUCTION

A recent report on superconducting hydrogen sulfide H_3S has opened the possibility of a new class of hydrogen-based high temperature superconductors [1]. High pressure studies enable one to access this class of superconductors, including proposed metallic hydrides [2]. Such studies have become a very active research area [3,4] with a reported measured T_C reaching 260 K in lanthanum hydrides [5–7]. Concurrent theoretical studies have also accelerated the search for new hydride superconductors: a number of different hydrogen-based superconductors have been suggested [8], some with a transition temperature remarkably above room temperature (e.g., 473 K of Li_2MgH_{16} at 250 GPa) [9]. Perhaps not surprising, a related search has focused on other light atom superconductors, including those based on doped carbon allotropes such as fullerenes [10], graphite [11], carbon nanotubes [12,13], and diamond [14–16]. Examples of such studies include a recent report claiming that a form of boron-doped disordered carbon, "*Q carbon*," exhibits superconductivity at rather large transition temperature [17–20]. This material's purported T_C is observed to be one of the highest among carbon-based materials, 55 K, achieved with a high concentration of boron atoms [18]. However, this T_C is not comparable to those of high-T_C cuprate superconductors [21].

Recently room temperature superconductivity has been reported in a ternary carbon-sulfur-hydrogen system with an equal ratio of carbon and sulfur atoms by Snider *et al.* [22]. Their results can be regarded not only as a record T_C hydride, but also as a new class of carbon-based superconductors. However, to the best of our knowledge, their report of room temperature superconductivity has not yet been confirmed by other researchers.

Theoretically, several candidate structures have been proposed for the ternary materials. Methane intercalated to a *R3m* hydrogen sulfide host crystal (H_7CS) is predicted to be a superconductor with 180–190 K at a relatively low pressure of 100–200 GPa [23,24]. Another theoretical study indicates a possible disagreement between theoretical predictions and the experimental results, despite the excellent agreement for predictions of superconductivity for the sulfur hydride and lanthanum hydride cases [25]. A thorough study on a number of H-C-S compositions showed a lowering of the DOS at the Fermi energy as the carbon content increases, suggesting the difficulty of high Tc conventional superconductivity in ternary materials [26].

Here, we study H-C-S ternary systems with various structures by focusing on systems with an equivalent ratio of carbon and sulfur atoms. We consider structures in a small unit cell with one formula unit of H_xCS and in a large unit cell with the composition of $H_{48}C_6S$. We also consider carbon hydride (H_xC) systems to investigate possible superconductivity. We choose these compositions to understand how carbon affects the superconductivity in hydrogen sulfide and also to find other potential carbon-based superconductors. Using pseudopotentials constructed within density functional theory, we obtain relatively high T_C structures in both H_xCS and H_xC. The structures examined in this work indicate no sign of a network between carbon and sulfur atoms mediated by hydrogen atoms. As such, our results fail to confirm a mechanism for carbon enhancing T_C in H-C-S ternary systems.

II. COMPUTATIONAL METHODS

We employ a total-energy pseudopotential method constructed within density functional theory [27–30]. We use a real-space pseudopotential code (PARSEC) with a grid spacing of 0.3 a. u. (1 a.u. = 0.5202 Å) to randomize the H-C-S systems. Owing to existing software implementations, we utilized a plane-wave basis (in QUANTUM ESPRESSO) for other parts of our simulations [31].

TABLE I. The number of unique optimized structures for each composition. Ten randomized structures were used as initial structures. Nonunique structures are eliminated by comparing the enthalpies of the structures. Here the densities of states at the Fermi energy [$N(E_F)$ is given in states/eV) are also listed. Here maximum, minimum, and average are taken among the same composition. The $N(E_F)$ listed here is computed from the density of states calculation with a finer k grid.

Composition	Number of structures	Maximum $N(E_F)$	Minimum $N(E_F)$	Average $N(E_F)$
H_6CS	7	0.666	0.185	0.425
H_7CS	9	0.632	0.321	0.461
H_8CS	10	0.483	0.241	0.396
H_9CS	9	0.541	0.288	0.468
$H_{10}CS$	9	0.615	0.000	0.390
H_6C_2	6	0.385	0.000	0.078
H_7C_2	5	0.298	0.176	0.225
H_8C_2	6	0.000	0.000	0.000
H_9C_2	6	0.558	0.162	0.298
$H_{10}C_2$	8	0.465	0.000	0.058

Troullier-Martins norm-conserving pseudopotentials and Vanderbilt ultrasoft pseudopotentials were both used in our work. We employed a generalized gradient approximation exchange-correlation energy functional proposed by Perdew, Burke, and Ernzerhof [32–34]. The cutoff energy for the wave function and the charge density is 40 and 400 Ry, respectively. We used density functional perturbation theory to compute phonon modes and electron-phonon coupling in H-C-S materials [31,35]. An electron-phonon line width for each phonon mode is calculated from the electron-phonon matrix elements [36]. A Gaussian broadening of 0.015–0.04 Ry is used to approximate δ functions, which appear in Brillouin zone summations of electron-phonon calculations. The width of broadening is chosen so that converged results were obtained. We compute the Eliashberg spectral function and electron-phonon coupling strength λ by using the electron-phonon line width. The superconducting transition temperature T_C is calculated from λ by using Allen-Dynes equation [37]. Here we use an effective Coulomb repulsion parameter μ^* of 0.10 for the best case scenario.

We initially perform a structural search with simple stoichiometries and small cells for H-C-S systems. The ratio between carbon and sulfur is fixed to 1:1 as reported in the experiment. We change the amount of hydrogen x of H_xCS from 6 to 10 in order to examine possible hydrogen compositions. For each composition, we generate 10 randomized structures. Each of the ten structures start from a random atomic distribution, save at least a 1-Å separation between atoms in a cubic box. The structure is then relaxed under a constant pressure of 250 GPa within a variable cell. Relaxation often gives a similar structure from different initial atomic coordinates. Unique selected structures are further investigated with a density of states calculation followed by electron-phonon simulations. For completeness, we also perform a structure search for H_xC_2 where x runs from 6 to 10. We place two carbon atoms in the simulation cell to make the comparison clear. A $16 \times 16 \times 16\,k$ grid is used for structural relaxation while a density of states (DOS) calculation is performed with a denser $24 \times 24 \times 24\,k$ grid. The electron-phonon coupling constant is computed with a combination of a $16 \times 16 \times 16\,k$ grid and a $4 \times 4 \times 4\,q$ grid.

We also consider several different structures of H-C-S ternary materials under a pressure of 250 GPa. We take a composition H_8CS so that enough hydrogen atoms are present so as to not overlook any signs of the formation of H-C-S networks because of the shortage of hydrogen atoms. Ten random structures of a 60 atom C_6S_6H system are generated in a cubic cell with a lattice constant of 8.2 Å. Initial atomic positions are completely randomized in a large cell.

The system is equilibrated using constant temperature Langevin molecular dynamics in a fixed box. Then, the structure is fully optimized in the same way as performed for the small cell. The atomic positions and cell parameters are fully relaxed under a pressure of 250 GPa. We further remove hydrogen molecules (H_2) from the resultant structure to assess the effect of the H_2 molecule on the superconducting properties. Structural relaxation is performed with a $8 \times 8 \times 8\,k$ grid. We use only Γ-point sampling for the q point of the electron-phonon calculations for the large cell. Superconducting properties are studied even when imaginary frequency mode appears. We estimate T_c by neglecting the contribution from the entire imaginary branch. This approach has been used previously [8,38] and should yield reasonable superconducting properties when the dynamical instabilities are removed.

We consider the relative stabilities of H_xCS and H_xC_2 as a function of hydrogen concentration using the enthalpy of formation H and pressure:

$$H(H_{x+1}CS) = H_{tot}(H_{x+1}CS) - H_{tot}(H_xCS) - \mu(H), \quad (1)$$

as an example expression for H_xCS. H_{tot} is the enthalpy at a pressure of 250 GPa. We adopt the enthalpy of *Cmca*-12 hydrogen as the reference chemical potential [μ(H)] of hydrogen under 250 GPa [39]. We consider only relative stabilities among the structures to explore the hydrogen concentration dependence of the enthalpy of formation.

III. RESULTS AND DISCUSSION

Table I lists the number of the unique structures for each composition obtained from the small randomized structures. Typically there are some nonunique structures in H_xC while

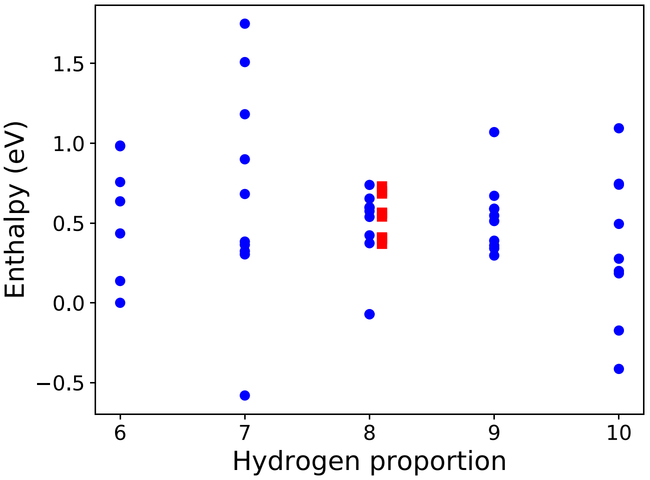

FIG. 1. Enthalpy of formation (eV) of H_xCS systems as a function of hydrogen proportion, defined in Eq. (1). Blue circles show the results obtained from the small cells while red squares at $x = 8.1$ show the enthalpy of the large cell with the composition of $H_{48}C_8S$. The chemical potential of hydrogen is taken as the enthalpy of the *Cmca*-12 structure of hydrogen. The zero in the plot is taken as the enthalpy of the lowest enthalpy structure of H_6CS.

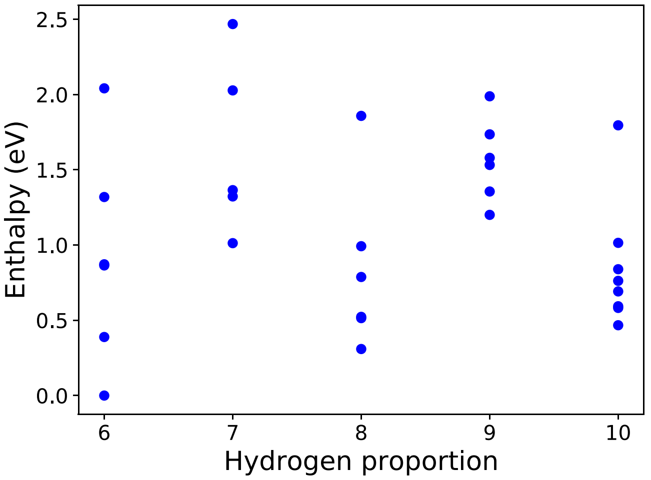

FIG. 2. Enthalpy of formation (eV) of H_xC_2 structures as a function of hydrogen proportion. The chemical potential of hydrogen is taken as *Cmca*-12 hydrogen structure. The zero of the plot is taken as the enthalpy of the lowest enthalpy structure of H_6C_2.

H_xCS gives mostly unique structures, except for the $x = 6$ case. This should arise from the more degrees of freedom in ternary H_xCS. Some of the structures obtained here have been reported in the literature. For example, the H7CS structure where the center sulfur atom of the body-centered-cubic H_3S is replaced with a methane (CH_4) molecule [23–25] is found in this work as well.

The densities of states are also listed in Table I. The electronic properties of H_xCS are mostly metallic, indicating the emergence of superconductivity. On the other hand, for the H_xC under 250 GPa, the H_6C, the H_8C, and the $H_{10}C$ cases are mostly insulating as C-C and C-H bond tends to saturate unpaired electrons with even numbers of hydrogen atoms. The only two exceptions are one in the case of H_6C and one in $H_{10}C$ where an unusual structural network is found. Otherwise similar atomic networks to those of general hydrocarbon molecules can be seen even under a pressure of 250 GPa, resulting in nonmetallic and nonsuperconducting properties. In contrast, those with an odd number of hydrogen atoms are metallic because of the ease of forming unpaired electrons.

The enthalpy of formation of H_xCS as a function of hydrogen proportion is shown in Fig 1. The previously found H_7CS structure with methane intercalated hydrogen sulfide has the lowest enthalpy among the all structures studied here. The enthalpy does not show a monotonic change as a function of the number of hydrogen atoms. We do not find a well-defined limit for the maximum hydrogen content in these systems. This agrees with a previous study showing a nonmonotonic change as a function of hydrogen content [25].

The enthalpy of formation as a function of hydrogen content for the H_xC_2 systems is shown in Fig. 2. In contrast to the previous H_xCS cases, this system does not favor an increase of the proportion of the hydrogen atoms if we separately note the odd-number and even number hydrogen content cases. The enthalpy for the odd-number hydrogen cases is relatively large when compared with even number cases. As we discussed earlier, the even number compositions are mostly insulating while the odd-number cases are metallic. The saturation of unpaired electrons in an insulator lowers the enthalpy.

We examine the phonon and electron-phonon properties of structures with the lowest enthalpy or the highest $N(E_F)$ in each composition, as the low enthalpy structures are most likely to be synthesized while the high $N(E_F)$ N(E_F) may contribute to high superconducting temperatures.

Table II presents the superconducting parameters of these selected structures. Here we list only structures without imaginary frequency modes or with only one imaginary phonon branches. Those with one imaginary frequency branch are marked with asterisk at their λ values. Superconducting properties are listed by neglecting the contribution from the imaginary phonon branch to assess the properties in these

TABLE II. Superconducting parameters of selected structures (with the highest density of states or with the lowest total energy) for H_xCS and H_xC_2. The electron phonon coupling strength λ, logarithmic average phonon frequency, $\omega_{\log}$, and superconducting transition temperatures are listed. Structures with two or more more imaginary modes are not listed here. The H_8C_2 structures are dismissed because they are all insulators. The $H_{10}C_2$ structures are also dismissed because the only metallic structure is dynamically unstable.

	Max. $N\ (E_F)$			Min. H_{tot}		
	λ	$\omega_{\log}$	T_C	λ	$\omega_{\log}$	T_C
H_6CS	1.99*	957	137	0.44	1090	7.4
H_7CS	–	–	–	1.20	1663	147
H_8CS	0.93*	1143	71	–	–	–
H_9CS	1.59	503	61	1.11*	1073	87
$H_{10}CS$	1.64*	1001	124	0.62*	1065	32
H_6C_2	2.41*	1067	172	–	–	–
H_7C_2	0.67*	1134	35	1.32*	852	85
H_9C_2	–	–	–	0.42*	1618	9.1

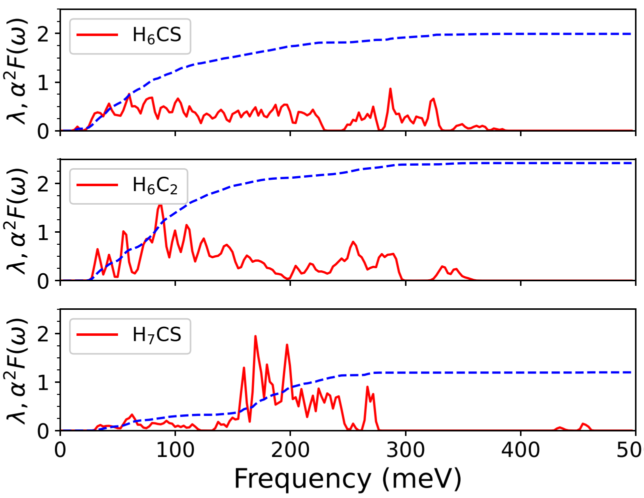

FIG. 3. Eliashberg spectral function (red solid lines) and cumulative electron-phonon coupling strength λ (blue dashed lines) as a function of phonon frequency (meV). Top, middle, and bottom panels correspond to H_6CS with T_C of 137 K, H_6C_2 with T_C of 172 K, and $R3m$ H_7CS with T_C of 149 K, respectively.

systems. Even low enthalpy structures show imaginary frequency phonon modes and are not dynamically stable. For example, the lowest enthalpy structure of H_8CS is fivefold coordinated methane intercalated hydrogen sulfide (one hydrogen atom added to the methane intercalated structure). The enthalpy is clearly lower than other H_8CS structures, but the over coordination is likely to exhibit an instability. In contrast, the high enthalpy structures with high $N(E_F)$ do not necessarily show dynamical instabilities.

The methane intercalated hydrogen sulfide H_7CS reported in the literature is confirmed to be stable with relatively high T_C of 149 K. Another dynamically stable structure is H_9CS with the highest $[N(E_F)]$ at this composition and shows the T_C of 61 K. Even though this structure is dynamically stable, the low $\omega_{\log}$ (503 K) implies the existence of strongly soften phonon modes and its instability. The other stable structure is the lowest enthalpy structure at H_6CS but its superconducting properties are not promising.

The H_xC_2 structures selected here are not dynamically stable in contrast to the above H_xCS cases. Interestingly the metallic H_6C_2 structures exhibit relatively high T_C of 172 K. The Eliashberg spectral function is shown in the middle panel of Fig 3. The contribution from low frequency modes are dominant when compared with the spectral function of $R3m$ H_7CS (see the bottom panel of Fig. 3). The middle frequency modes (200–300 meV) in H_7CS execute scissorlike motion involving both hydrogen atoms bonded to sulfur and carbon atoms. The contribution from hydrogen stretching modes is very limited (relevant frequencies are above 400 meV). On the other hand soft CH stretching modes mixed with other motions contributes to the $\alpha^2F(\omega)$ in the case of H_6C_2. The same trend applies to H_6CS. These structures are not dynamically stable, but a further structure search might find a stable structure with interesting superconducting properties.

The selected structures are illustrated in Fig. 4. Figures 4(a)–4(c) are the structures of H_xCS. Sulfur atoms and hydrogen atoms form a network in the dynamically stable structure H_9CS shown in Fig. 4(b) while the hydrocarbon can be seen as a guest intercalated to this sulfur-hydrogen network. This guest-host relationship is similar to the stable methane-intercalated hydrogen sulfide H_7CS [25]. In other high T_C but dynamically unstable structures, carbon and sulfur

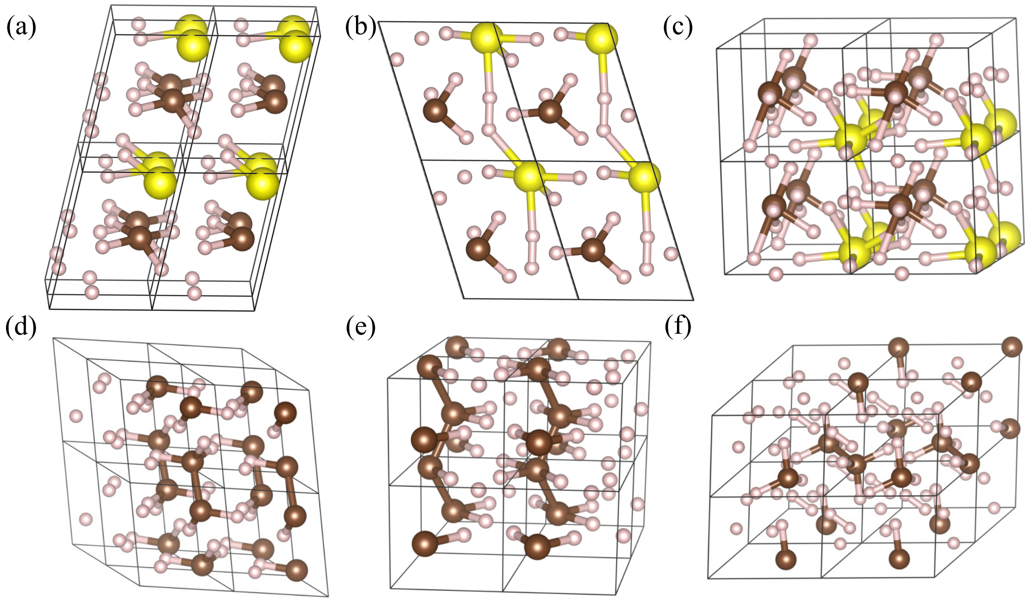

FIG. 4. Ball-and-stick model structures of (a) dynamically unstable but high T_C H_6CS, (b) dynamically stable H_9CS, and (c) another unstable but high T_C $H_{10}CS$. The structures of (d) insulating H_6C_2, (e) metallic H_6C_2, and (f) insulating $H_{10}C_2$ are also illustrated. White, brown, and yellow spheres represent hydrogen, carbon, and sulfur atoms, respectively. The VESTA software is used to generate images [40]. The lattice parameters and atomic coordinates of these structures are provided in Supplemental Material [41].

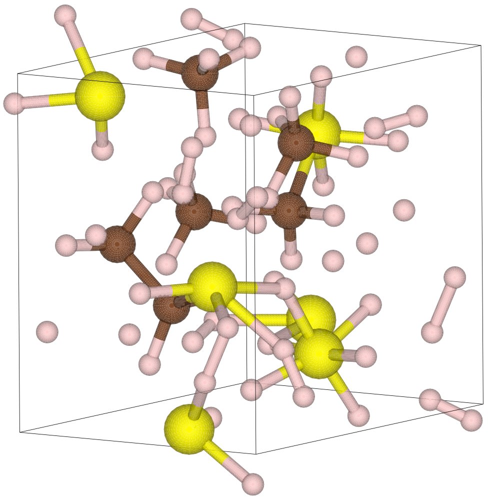

FIG. 5. Fully optimized ball-and-stick model structure of $H_{48}C_6S$ with the lowest enthalpy among 10 structures. Atoms outside the cell are also illustrated when these atoms form bonds with the atoms inside the cell. White, brown, and yellow spheres represent hydrogen, carbon, and sulfur atoms, respectively. The lattice parameters and atomic coordinates of this structures are provided in Supplemental Material [41].

atoms also do not form any network like H_3S where sulfur atoms are connected through hydrogen atoms. This indicates that carbon and sulfur atoms are rather isolated with each other than form the effective structure to realize high T_C under a high pressure.

Figure 4(d) illustrates the structure of insulating H_6C_2. Here carbon and hydrogen atoms form ethane like molecules. There are no unpaired electrons and no network is formed between carbon atoms through hydrogen atoms. When more hydrogen atoms are incorporated, the insulating tendency does not change. The structure of $H_{10}C_2$ shown in Fig. 4 contains extra hydrogen molecules and no metallic properties are observed. Low enthalpy is achieved by forming noninteracting molecules even with the high pressure. On the other hand, the metallic H_6C_2 shown in Fig. 4(e) have carbon atoms in the unusual fivefold coordination. Although the enthalpy is high and the structure is dynamically unstable, it is interesting to see the relatively high superconducting temperature in this fivefold coordinated network of carbon and hydrogen atoms.

The structures discussed above have a relatively small unit cell and as a consequence may contain some correlated structural elements. This issue can be mitigated by increasing the cell size. This made is apparent by increasing the cell size to contain 60 atoms as shown in Fig. 5. Despite the change in cell size, the enthalpy of formation is well within the range of the enthalpy of the small-cell structures. The tendency of the formation of S-H network as for H_3S remains independent of the formation of hydrogen and hydrocarbon molecules and is consistent with the small-cell study. This confirms the lack of a C-H-S network in the ternary system even under high pressure. We note that a similar difficulty in forming networks among carbon and sulfur atoms, even under pressure, has been previously reported and discussed in the literature [42].

In brief, two of our studied structures are insulating. Of the metallic structures, the maximum, minimum, and average densities of states among are 1.55, 0.139, and 0.806 states/eV/cell, respectively. The highest and the lowest T_C among the 10 structures is 76 and 46 K, respectively. The average T_C of the metallic structures is 64 K, indicating no large deviation in T_C. The consistent and low value of T_C confirms the difficulty in obtaining a room temperature value for this system by the addition of C atoms.

IV. SUMMARY

In summary, we examined H-C-S materials with various compositions. The most stable and realistic H_xCS material with a high T_C is the previously reported $R3m$ H_7CS where methane molecules are intercalated into the hydrogen sulfide host. Based on the structures studied here, carbon and sulfur atoms do not form a network through hydrogen atoms, indicating that introducing carbon into hydrogen sulfide does not promote superconductivity. H_xC_2 systems are mostly insulating, but unusual coordination can lead to metallic and superconducting properties with relatively high T_C. Although the high T_C H_6C_2 studied here are not dynamically stable, we expect further structural searches could find a similar structure with dynamical stabilities.

ACKNOWLEDGMENTS

Y.S. and J.R.C. acknowledge support from the U.S. Department of Energy (DOE) on a subaward from the Center for Computational Study of Excited-State Phenomena in Energy Materials at the Lawrence Berkeley National Laboratory, which is funded by the U.S. Department of Energy, Office of Science, Basic Energy Sciences, Materials Sciences and Engineering Division under Contract No. DE-AC02-05CH11231, as part of the Computational Materials Sciences Program. Computational resources are provided in part by the National Energy Research Scientific Computing Center (NERSC) and Texas Advanced Computing Center (TACC). M.L.C. acknowledges the National Science Foundation Grant No. DMR-1926004 support for research associated with conceptualizing and developing the theory and from the Theory of Materials Program at the Lawrence Berkeley National Laboratory funded by the Director, Office of Science and Office of Basic Energy Sciences, Materials Sciences and Engineering Division, U.S. Department of Energy under Contract No. DE-AC02-05CH11231 for supporting research related to the computational aspects involved in this project.

---

[1] A. P. Drozdov, M. I. Ermets, I. A. Troyan, V. Ksenofontov, and S. I. Shylin, Nature (London) **525**, 73 (2015).
[2] N. W. Ashcroft, Phys. Rev. Lett. **92**, 187002 (2004).
[3] J. A. Flores-Livas, L. Boeri, A. Sanna, G. Profeta, R. Arita, and M. Eremets, Phys. Rep. **856**, 1 (2020).
[4] C. J. Pickard, I. Errea, and M. I. Eremets, Annu. Rev. Condens. Matter Phys. **11**, 57 (2020).

[5] A. P. Drozdov, P. P. Kong, V. S. Minkov, S. P. Besedin, M. A. Kuzovnikov, S. Mozaffari, L. Balicas, F. F. Balakirev, D. E. Graf, V. B. Prakapenka, E. Greenberg, D. A. Knyazev, M. Tkacz, and M. I. Eremets, Nature (London) **569**, 528 (2019).

[6] M. Somayazulu, M. Ahart, A. K. Mishra, Z. M. Geballe, M. Baldini, Y. Meng, V. V. Struzhkin, and R. J. Hemley, Phys. Rev. Lett. **122**, 027001 (2019).

[7] I. Errea, F. Belli, L. Monacelli, A. Sanna, T. Koretsune, T. Tadano, R. Bianco, M. Calandra, R. Arita, F. Mauri, and J. A. Flores-Livas, Nature (London) **578**, 66 (2020).

[8] A. M. Shipley, M. J. Hutcheon, R. J. Needs, and C. J. Pickard, Phys. Rev. B **104**, 054501 (2021).

[9] Y. Sun, J. Lv, Y. Xie, H. Liu, and Y. Ma, Phys. Rev. Lett. **123**, 097001 (2019).

[10] K. Tanigaki, T. W. Ebbesen, S. Saito, J. Mizuki, J. S. Tsai, Y. Kubo, and S. Kuroshima, Nature (London) **352**, 222 (1991).

[11] T. E. Weller, M. Ellerby, S. S. Saxena, R. P. Smith, and N. T. Skipper, Nat. Phys. **1**, 39 (2005).

[12] N. Murata, J. Haruyama, J. Reppert, A. M. Rao, T. Koretsune, S. Saito, M. Matsudaira, and Y. Yagi, Phys. Rev. Lett. **101**, 027002 (2008).

[13] J. Haruyama, M. Matsudaira, J. Reppert, A. Rao, T. Koretsune, S. Saito, H. Sano, and Y. Iye, J. Supercond. Nov. Magn. **24**, 111 (2011).

[14] E. A. Ekimov, V. A. Sidorov, E. D. Bauer, N. N. Mel'nik, N. J. Curro, J. D. Thompson, and S. M. Stishov, Nature (London) **428**, 542 (2004).

[15] Y. Takano, T. Takenouchi, S. Ishii, S. Ueda, T. Okutsu, I. Sakaguchi, H. Umezawa, H. Kawarada, and M. Tachiki, Diamond Relat. Mater. **16**, 911 (2007).

[16] H. Okazaki, T. Wakita, T. Muro, T. Nakamura, Y. Muraoka, T. Yokoya, S. Kurihara, H. Kawarada, and T. Oguchi, Appl. Phys. Lett. **106**, 052601 (2015).

[17] A. Bhaumik, R. Sachan, and J. Narayan, ACS Nano **11**, 5351 (2017).

[18] A. Bhaumik, R. Sachan, S. Gupta, and J. Narayan, ACS Nano **11**, 11915 (2017).

[19] J. Narayan and A. Bhaumik, J. Appl. Phys. **118**, 215303 (2015).

[20] Y. Sakai, J. R. Chelikowsky, and M. L. Cohen, Phys. Rev. B **97**, 054501 (2018).

[21] A. Schilling, M. Cantoni, J. D. Guo, and H. R. Ott, Nature (London) **363**, 56 (1993).

[22] E. Snider, N. Dasenbrock-Gammon, R. McBride, M. Debessai, H. Vindana, K. Vencatasamy, K. V. Lawler, A. Salamat, and R. P. Dias, Nature (London) **586**, 373 (2020).

[23] Y. Sun, Y. Tian, B. Jiang, X. Li, H. Li, T. Iitaka, X. Zhong, and Y. Xie, Phys. Rev. B **101**, 174102 (2020).

[24] W. Cui, T. Bi, J. Shi, Y. Li, H. Liu, E. Zurek, and R. J. Hemley, Phys. Rev. B **101**, 134504 (2020).

[25] T. Wang, M. Hirayama, T. Nomoto, T. Koretsune, R. Arita, and J. A. Flores-Livas, Phys. Rev. B **104**, 064510 (2021).

[26] M. Gubler, J. A. Flores-Livas, A. Kozhevnikov, and S. Goedecker, Phys. Rev. Materials **6**, 014801 (2022).

[27] J. Ihm, A. Zunger, and M. L. Cohen, J. Phys. C **12**, 4409 (1979).

[28] M. L. Cohen, Phys. Scr. **T1**, 5 (1982).

[29] P. Hohenberg and W. Kohn, Phys. Rev. **136**, B864 (1964).

[30] W. Kohn and L. J. Sham, Phys. Rev. **140**, A1133 (1965).

[31] P. Giannozzi, S. Baroni, N. Bonini, M. Calandra, R. Car, C. Cavazzoni, D. Ceresoli, G. L. Chiarotti, M. Cococcioni, I. Dabo, A. Dal Corso, S. de Gironcoli, S. Fabris, G. Fratesi, R. Gebauer, U. Gerstmann, C. Gougoussis, A. Kokalj, M. Lazzeri, L. Martin-Samos, N. Marzari, F. Mauri, R. Mazzarello, S. Paolini, A. Pasquarello, L. Paulatto, C. Sbraccia, S. Scandolo, G. Sclauzero, A. P. Seitsonen, A. Smogunov, P. Umari, and R. M. Wentzcovitch, J. Phys. Condens. Matter **21**, 395502 (2009).

[32] N. Troullier and J. L. Martins, Phys. Rev. B **43**, 1993 (1991).

[33] D. Vanderbilt, Phys. Rev. B **41**, 7892 (1990).

[34] J. P. Perdew, K. Burke, and M. Ernzerhof, Phys. Rev. Lett. **77**, 3865 (1996).

[35] S. Baroni, S. de Gironcoli, A. dal Corso, and P. Giannozzi, Rev. Mod. Phys. **73**, 515 (2001).

[36] F. Giustino, Rev. Mod. Phys. **89**, 015003 (2017).

[37] P. B. Allen and R. C. Dynes, Phys. Rev. B **12**, 905 (1975).

[38] K. Nakano, K. Hongo, and R. Maezono, Sci. Rep. **6**, 29661 (2016).

[39] C. J. Pickard and R. J. Needs, Nat. Phys. **3**, 473 (2007).

[40] K. Momma and F. Izumi, J. Appl. Crystallogr. **44**, 1272 (2011).

[41] See Supplemental Material at http://link.aps.org/supplemental/10.1103/PhysRevMaterials.6.044801 for the details of the structures presented here.

[42] S. S. Naghavi, Y. Crespo, R. Martoňák, and E. Tosatti, Phys. Rev. B **91**, 224108 (2015).